© 2016. Published by The Company of Biologists Ltd | Journal of Cell Science (2016) 129, 1580-1591 doi:10.1242/jcs.182097

RESEARCH ARTICLE

Oxidized LDL induces FAK-dependent RSK signaling to drive NF-κB activation and VCAM-1 expression

Arif Yurdagul, Jr[1,2], Florian J. Sulzmaier[3], Xiao L. Chen[3,4], Christopher B. Pattillo[5], David D. Schlaepfer[3] and A. Wayne Orr[1,2,*]

ABSTRACT

Oxidized low-density lipoprotein (oxLDL) accumulates early in atherosclerosis and promotes endothelial nuclear factor κB (NF-κB) activation, proinflammatory gene expression and monocyte adhesion. Like for other atherogenic factors, oxLDL-induced proinflammatory responses requires integrin-dependent focal adhesion kinase (FAK, also known as PTK2) signaling; however, the mechanism by which FAK mediates oxLDL-dependent NF-κB signaling has yet to be revealed. We now show that oxLDL induces NF-κB activation and VCAM-1 expression through FAK-dependent IκB kinase β (IKKβ, also known as IKBKB) activation. We further identify FAK-dependent activation of p90 ribosomal S6 kinase family proteins (RSK) as a crucial mediator of oxLDL-dependent IKKβ and NF-κB signaling, as inhibiting RSK blocks oxLDL-induced IKKβ and NF-κB activation, VCAM-1 expression and monocyte adhesion. Finally, transgenic mice containing a kinase-dead mutation in FAK specifically in the endothelial cells show reduced RSK activity, decreased VCAM-1 expression and reduced macrophage accumulation in regions of early atherosclerosis. Taken together, our data elucidates a new mechanism whereby oxLDL-induced endothelial FAK signaling drives an ERK–RSK pathway to activate IKKβ and NF-κB signaling and proinflammatory gene expression.

KEY WORDS: Focal adhesion kinase, FAK, OxLDL, Oxidized LDL, Ribosomal S6 kinase, RSK, Nuclear factor κB, NF-κB, Atherosclerosis

INTRODUCTION

During early atherosclerosis, low-density lipoproteins (LDLs) accumulate in medium- and large-sized arteries of the vasculature as native LDL particles. However, rising levels of oxidative stress promote LDL oxidation (Goyal et al., 2012). Oxidized LDL (OxLDL) binding to scavenger receptors drives endothelial cell activation, a phenotype characterized by enhanced permeability and proinflammatory gene expression (Xu et al., 2013). This change in endothelial cell phenotype requires the activation of transcription factors, such as nuclear factor-κB (NF-κB), that evoke proinflammatory adhesion molecule expression, such as E-selectin, vascular cell adhesion molecule-1 (VCAM-1) and intercellular adhesion molecule-1 (ICAM-1). This alteration in endothelial cell function by NF-κB signaling results in enhanced inflammatory cell recruitment and primes the development of atherosclerosis (Libby et al., 2011).

NF-κB activation in endothelial cells plays a central role in modulating gene expression by multiple atherogenic factors (Sun and Andersson, 2002). In quiescent cells, the inhibitor of NF-κB (IκB) proteins sequester NF-κB in the cytosol. Upon stimulation with inflammatory mediators, IκB kinase β (IKKβ, also known as IKBKB) phosphorylates IκB resulting in its ubiquitylation and proteosomal degradation, thereby allowing NF-κB nuclear translocation and transcription (Lawrence, 2009). IKKβ also phosphorylates the p65 subunit of NF-κB (RelA, hereafter just NF-κB) on S536, which is crucial for maximal NF-κB-dependent gene expression (Lawrence, 2009). Alternatively, NF-κB can be induced by IKK-independent pathways, such as oxidative-stress-induced tyrosine phosphorylation of IκB proteins resulting in NF-κB release and nuclear translocation without IκB degradation (Sun, 2011; Takada et al., 2003). However, physiological levels of oxidative stress can also activate classic IKK-dependent NF-κB signaling as well (Gloire et al., 2006). Although oxLDL elicits production of reactive oxygen species (ROS) in endothelial cells, serine-phosphorylation-deficient IκBα mutants diminish oxLDL-induced VCAM-1 expression, suggesting that an IKK-dependent mechanism is involved (Robbesyn et al., 2004; Valente et al., 2014; Yurdagul et al., 2014). However, the role of IKKβ or its upstream kinases in oxLDL-induced NF-κB activation remains unknown.

Multiple proinflammatory stimuli, including oxLDL, shear stress and TNFα (also known as TNF), promote NF-κB activation through the non-receptor tyrosine kinase focal adhesion kinase (FAK, also known as PTK2) (Funakoshi-Tago et al., 2003; Lim et al., 2012; Petzold et al., 2009; Yurdagul et al., 2014). FAK activation involves integrin ligation to the extracellular matrix, and inhibiting FAK activity reduces shear stress, TNFα and oxLDL-induced NF-κB activity and proinflammatory gene expression (Funakoshi-Tago et al., 2003; Lim et al., 2012; Petzold et al., 2009; Yurdagul et al., 2014). Although blocking FAK activity reduces endothelial cell activation, the involvement of FAK in proinflammatory responses varies in a context-dependent manner. For instance, FAK does not influence TNFα-induced NF-κB activity directly but instead localizes to the nucleus upon inhibition and regulates degradation of GATA4, a transcriptional regulator of VCAM-1 expression (Lim et al., 2012). Preventing shear-stress-induced FAK activation does not affect IκB degradation or nuclear translocation of NF-κB, but is essential for NF-κB phosphorylation and NF-κB-dependent expression of ICAM-1 (Petzold et al., 2009). In contrast, inhibiting FAK reduces the amount of oxLDL-induced NF-κB phosphorylation and nuclear translocation, suggesting another mechanism exists to account for the role of FAK in oxLDL-induced endothelial cell activation (Yurdagul et al., 2014).

[1]Department of Pathology and Translational Pathobiology, LSU Health Sciences Center, Shreveport, LA 71130, USA. [2]Department of Cell Biology and Anatomy, LSU Health Sciences Center, Shreveport, LA 71130, USA. [3]UCSD San Diego, Moores Cancer Center, Department of Reproductive Medicine, 0803 3855 Health Sciences Dr., La Jolla, CA 92093, USA. [4]State Key Laboratory of Cellular Stress Biology, Innovation Center for Cell Signaling Network, School of Life Sciences, Xiamen University, Xiamen, Fujian 361102, China. [5]Department of Cellular and Molecular Physiology, LSU Health Sciences Center, Shreveport, LA 71130, USA.

*Author for correspondence (aorr@lsuhsc.edu)

Received 16 October 2015; Accepted 14 February 2016

Journal of Cell Science (2016) 129, 1580-1591 doi:10.1242/jcs.182097

Therefore, we sought to delineate the mechanism of oxLDL-induced NF-κB activation through FAK signaling.

RESULTS

To determine whether oxLDL induces classic NF-κB signaling through IKKβ, we performed an IKKβ activity assay whereby immunoprecipitated IKKβ phosphorylates recombinant IκBα (also known as NFKBIA). Endothelial cells treated with 100 µg/ml of oxLDL showed a 2-fold and 1.7-fold increase in IKKβ activation at 30 and 60 min, respectively (Fig. 1A). We further investigated whether oxLDL drives exit of FAK from the nucleus given that it has been previously reported that FAK inhibition drives FAK nuclear localization and proteosomal degradation of GATA4, a VCAM-1 transcription factor. We found that oxLDL treatment did not elicit FAK emigration from the nucleus, excluding the possibility that oxLDL is increasing GATA4 levels in the nucleus (Fig. S1A). Furthermore, two different IKKβ-targeted small interfering RNAs (siRNAs; giving ∼85% knockdown) reduced oxLDL-induced NF-κB phosphorylation, nuclear translocation and VCAM-1 expression (Fig. 1B–E; Fig. S1B,C), suggesting that classical NF-κB signaling through IKKβ mediates the proinflammatory responses to oxLDL. Using the FAK kinase inhibitor PF-573228 or FAK-targeted siRNA (90% knockdown) significantly reduced oxLDL-induced IKKβ activity (Fig. 1F,G). However, FAK immunoprecipitates lacked IKKβ co-precipitation and IKKβ kinase activity (Fig. S1D,E), suggesting that an intermediate acts between FAK and IKKβ activation.

To identify the kinase involved in oxLDL-induced IKKβ activation, we used siRNA knockdown to screen multiple known IKKβ kinases, including receptor-interacting protein kinase 1 (RIP1, also known as RIPK1), transforming growth factor activated kinase 1 (TAK1, also known as MAP3K7), NF-κB-inducing kinase (NIK, also known as MAP3K14) and ribosomal S6 kinase (RSK1 and RSK2, also known as RPS6KA1 and RPS6KA3, respectively). However, only RSK knockdown reduced the oxLDL-induced NF-κB activation (Fig. 2A). Both RSK1 and RSK2 siRNAs were utilized in these experiments given that these two isoforms have been demonstrated to exhibit redundant functions. RSK proteins contain a C-terminal kinase domain (CTKD) and an N-terminal kinase domain (NTKD), which are connected by a linker region (Anjum and Blenis, 2008). Activation of RSK proteins is associated with CTKD-mediated phosphorylation of S380, and oxLDL treatment promoted a rapid and substantial phosphorylation at S380 (Fig. 2B). To test whether RSK promotes NF-κB activation through IKKβ, we utilized a small-molecule inhibitor of RSK proteins (BI-D1870) or targeted siRNA and performed IKKβ activity assays. We show that inhibition or loss of RSK significantly reduced oxLDL-induced IKKβ activity, supporting the role of RSK in IKKβ activation (Fig. 2C,D). Treatment with the FAK inhibitor PF-573228 completely inhibited both oxLDL-induced FAK and RSK phosphorylation (Fig. 2E). HAECs transfected with FAK-targeted siRNA reduced the amount of RSK activation induced by oxLDL (Fig. 2F). Moreover, primary mouse lung endothelial cells (MLECs) isolated from the lungs of transgenic mice with a FAK kinase-dead knock-in mutation showed significantly reduced levels of oxLDL-induced RSK activation compared to wild-type controls (Fig. 2G). Taken together, these data identify RSK as a new downstream effector of FAK that mediates IKKβ activation.

We next tested whether inhibiting RSK could reduce NF-κB activation and proinflammatory gene expression. BI-D1870 treatment significantly reduced oxLDL-mediated NF-κB activation, nuclear localization and VCAM-1 expression (Fig. 3A,D; Fig. S2A,B). Consistent with this, two different RSK-targeting siRNAs (∼75% knockdown) similarly diminished oxLDL-induced NF-κB phosphorylation, nuclear translocation and VCAM-1 expression (Fig. 3B,E; Fig. S1B,C). Furthermore, transfecting endothelial cells with a dominant-negative form of RSK (K94A and K447A mutations) reduced NF-κB and VCAM-1 luciferase reporter activity (Fig. 3C,F). Given that leukocytes populate a majority of atherosclerotic lesions and enhanced VCAM-1 expression mediates leukocyte adhesion, we next tested whether RSK plays a role in monocyte adhesion using the THP-1 monocyte cell line. Although oxLDL stimulates a robust increase in monocyte binding, inhibiting RSK with BI-D1870 or reducing RSK levels with siRNA significantly lowered oxLDL-induced monocyte adhesion (Fig. 3G,H).

RSK activation classically involves oxidative stress and activation of the ERK pathway. Given that oxLDL elicits robust increases in reactive oxygen species (ROS), we next examined whether the enhanced ROS levels stimulated by oxLDL were dependent on integrin signaling or FAK activity. Preventing integrin ligation (by use of integrin-α5-blocking antibodies) or FAK signaling (by treatment with PF-573228) did not significantly influence oxLDL-induced ROS production, as measured with 2',7'-dichlorofluorescin diacetate (DCFDA) (Fig. S2C,D). Furthermore, scavenging the free-radical superoxide did not block oxLDL-induced FAK activation (Fig. S3C), suggesting that the ROS production did not influence oxLDL-induced FAK signaling. Thus, the reduction seen upon inhibiting FAK on RSK activity are likely independent of changes in oxidative stress induced by oxLDL. Full RSK activity requires ERK-dependent phosphorylation in the C-terminal kinase domain. Given that FAK has been shown to mediate integrin-dependent ERK1 and ERK2 (ERK1/2, also known as MAPK3 and MAPK1, respectively) signaling, and oxLDL stimulates ERK1/2 activity, we next investigated the role of FAK in oxLDL-dependent ERK1/2 activation (Tanigawa et al., 2006). Using the FAK inhibitor PF-573228, we demonstrate that oxLDL-induced ERK1/2 activity requires FAK signaling (Fig. 4A). Strikingly, blocking ERK1/2 activity using the MEK inhibitor U0126, completely prevented oxLDL-induced RSK phosphorylation (Fig. 4B). Furthermore, we further demonstrate that inhibiting ERK1/2 signaling diminished oxLDL-induced NF-κB activation, nuclear localization, VCAM-1 expression and monocyte adhesion (Fig. 4C–H). Induction of ERK signaling by FAK corresponded with both FAK recruitment of the classic ERK pathway mediator Grb2 and FAK phosphorylation on Y925, the classic Grb2-interacting site (Fig. S3), suggesting that Grb2 might play an important role in mediating this pathway. Importantly, overexpression of a constitutively active FAK mildly enhanced ERK phosphorylation but did not influence RSK or NF-κB activation or VCAM-1 expression. This suggests that FAK is required for oxLDL-induced inflammatory signaling but is not sufficient (Fig. S4). Taken together, these data suggest that oxLDL promotes FAK-dependent ERK activation, resulting in RSK-mediated signaling to IKKβ and NF-κB.

Given that FAK regulates endothelial cell activation *in vitro*, we next tested whether FAK activation could be observed in endothelial cells overlying atherosclerotic plaques *in vivo*. We compared staining of FAK phosphorylated at Y397 (FAK-pY397) in normal, quiescent regions of the vasculature to that in regions positive for atherosclerosis (identified by macrophage staining) in brachiocephalic arteries from ApoE$^{-/-}$ mice fed a high-fat Western diet for 8 weeks. In regions with no plaque, some active FAK staining was apparent in the vessel media and adventitia, whereas

Journal of Cell Science (2016) 129, 1580-1591 doi:10.1242/jcs.182097

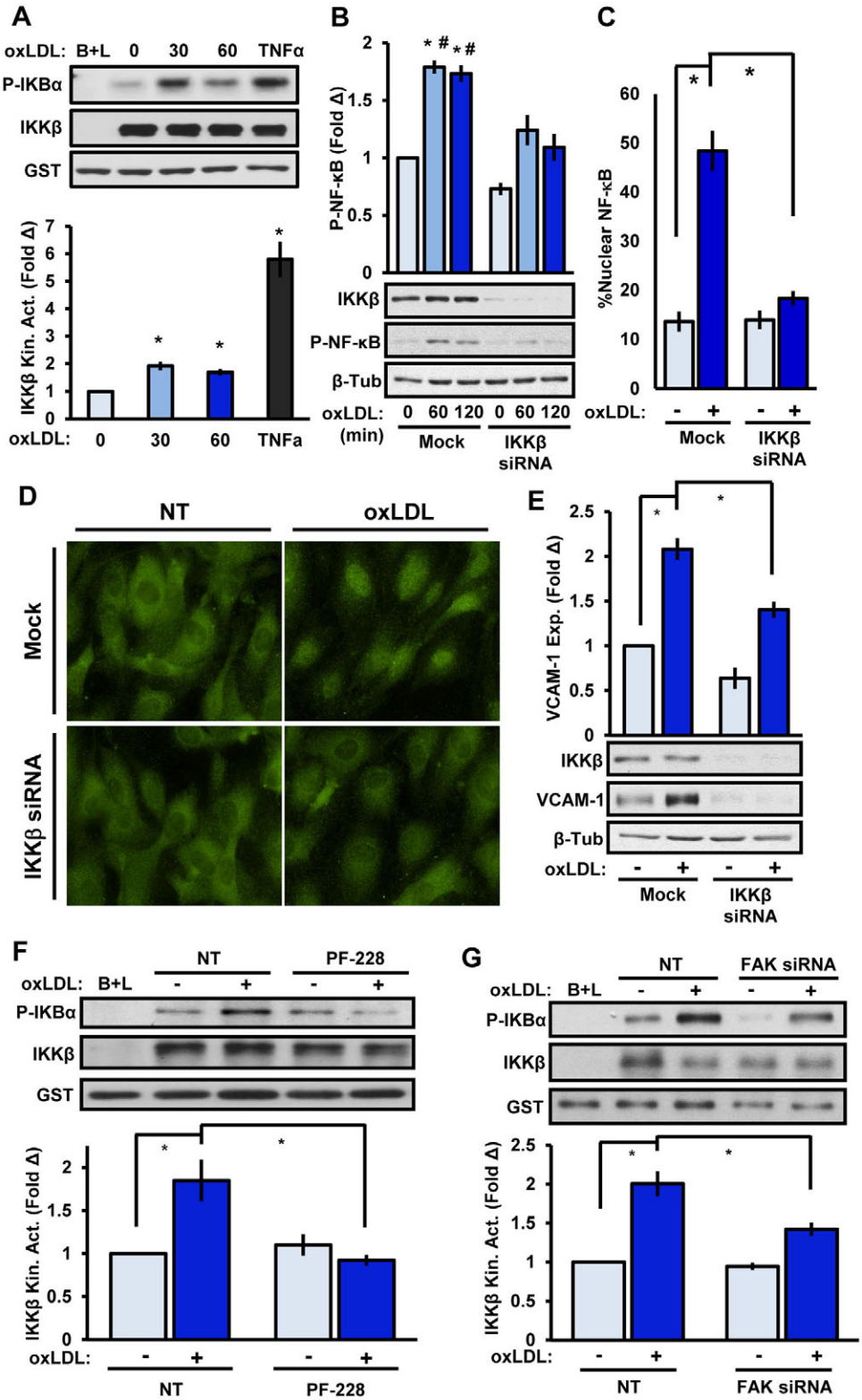

Fig. 1. OxLDL stimulates classic NF-κB activation through FAK. (A) IKKβ kinase activity (Kin. Act.) in HAE cells treated with oxLDL (100 µg/ml) for the indicated times or with TNFα (1 ng/ml) for 10 min. Beads plus lysate (B+L) served as a negative control and IKKβ activity is expressed as the mean±s.e.m. fold change (Δ) compared to unstimulated conditions (n=4). (B–E) Endothelial cells were transfected with IKKβ siRNA and oxLDL-induced (B) NF-κB phosphorylation (P-NF-κB; 60–120 min, immunoblotting), (C,D) nuclear translocation (60 min, p65 immunocytochemistry), or (E) VCAM-1 expression (exp., 6 h, immunoblotting) was determined. For nuclear translocation, at least 100 cells were scored for NF-κB positivity per condition for each experiment (n=4). (F,G) FAK signaling in HAE cells was inhibited with (F) PF-573228 (4 µM, 1 h) or (G) FAK siRNA and oxLDL-induced IKKβ kinase activity was assessed (n=4). Results are mean±s.e.m. *P<0.05 (compared to 0 time or no treatment) and $^{\#}P$<0.05 (compared to respective timepoint) using either (A) one-way ANOVA or (B–G) two-way ANOVA with Bonferroni post-hoc test. NT, no treatment. Mock indicates the mock transfection.

endothelial cells showed little to no active FAK staining. In contrast, endothelial cells overlying atherosclerotic plaques showed elevated active FAK staining (Fig. 5A,C). Similarly, human coronary arteries showed similar patterns of active FAK staining, with minimal active FAK in healthy areas and elevated active FAK in endothelial cells overlying atherosclerotic plaques (Fig. 5B,D). These data indicate that FAK activation is not only induced by various atherogenic stimuli in endothelial cells *in vitro*, but that endothelial FAK activation is increased during atherosclerotic disease progression.

To test the relevance of FAK *in vivo* and bypass the lethality of inactive FAK expression, we used transgenic mice containing a kinase-dead FAK knock-in allele (denoted KD), which prevents FAK activity but retains scaffolding functions. $FAK^{WT/flox}$

Journal of Cell Science (2016) 129, 1580-1591 doi:10.1242/jcs.182097

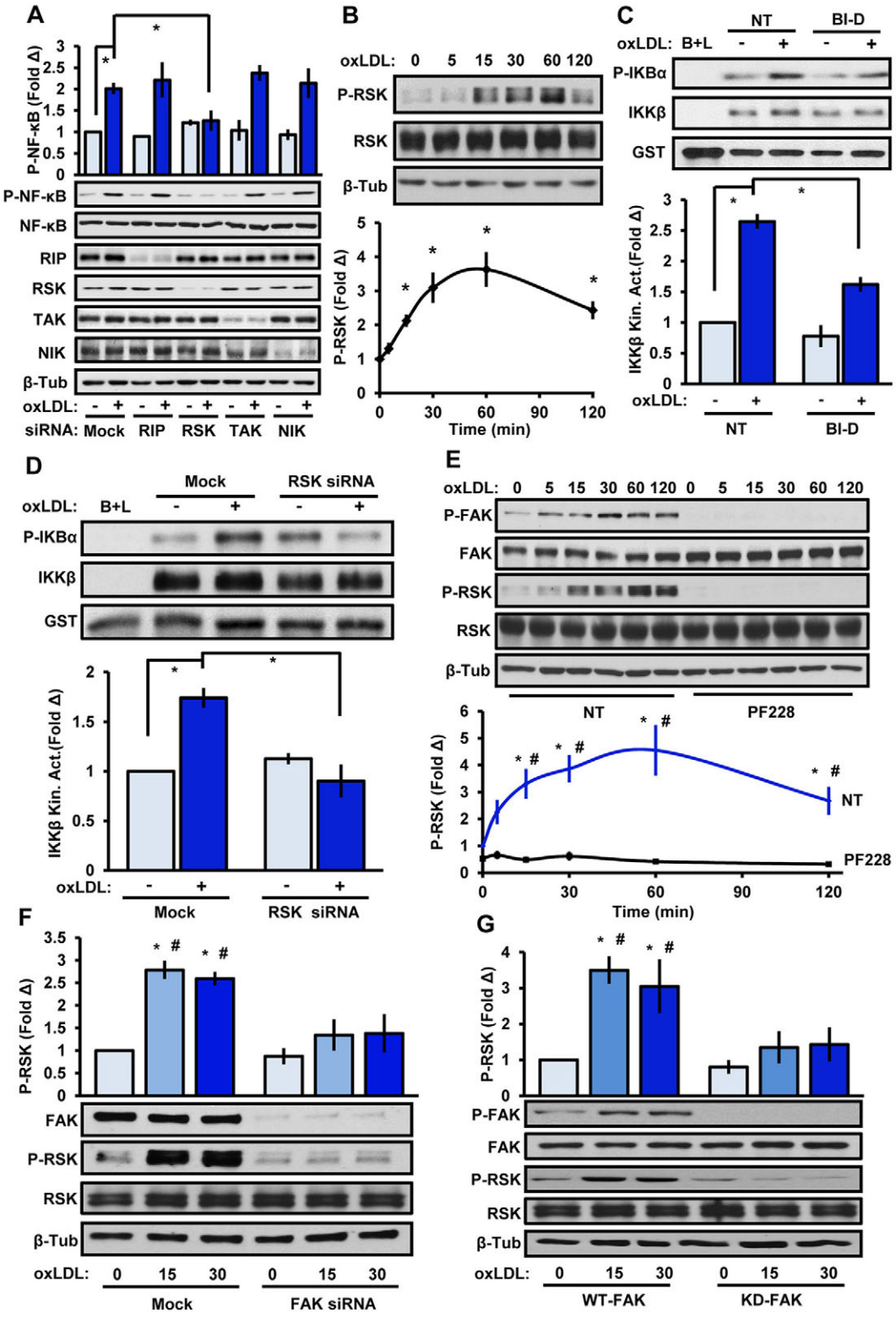

Fig. 2. RSK couples FAK signaling to IKKβ activation. (A) Endothelial cells transfected with siRNA targeting RIP, both RSK1 and RSK2, TAK or NIK were treated with oxLDL and NF-κB phosphorylation (P-NF-κB) was determined by immunoblotting (n=4). (B) Endothelial cells were treated with oxLDL for the indicated times and RSK phosphorylation (P-RSK) was determined by immunoblotting (n=5). (C,D) OxLDL-induced IKKβ kinase activity was determined. (C) Cells were pretreated with BI-D1870 (BI-D, 5 µM, 1 h) or (D) transfected with RSK1 and RSK2 siRNA. Results are mean±s.e.m. (n=4). (E,F) FAK signaling in HAE cells was inhibited with (E) PF-573228 (4 µM, 1 h) or (F) FAK siRNA, and oxLDL-induced (100 µg/ml; indicated timepoints) phosphorylation of FAK and RSK was determined by immunoblotting (n=4–5). (G) Primary lung endothelial cells isolated from FAK-WT or FAK-KD transgenic mice were treated with oxLDL for 15 or 30 min, and FAK and RSK phosphorylation was assessed by immunoblotting (n=5). Results are mean±s.e.m. $^{*}P$<0.05 (compared to 0 time or no treatment) or $^{\#}P$<0.05 (compared to respective timepoint) using either (B) one-way ANOVA or (A,C–G) two-way ANOVA with Bonferroni post-hoc test. NT, no treatment. Mock indicates mock transfection.

Journal of Cell Science (2016) 129, 1580-1591 doi:10.1242/jcs.182097

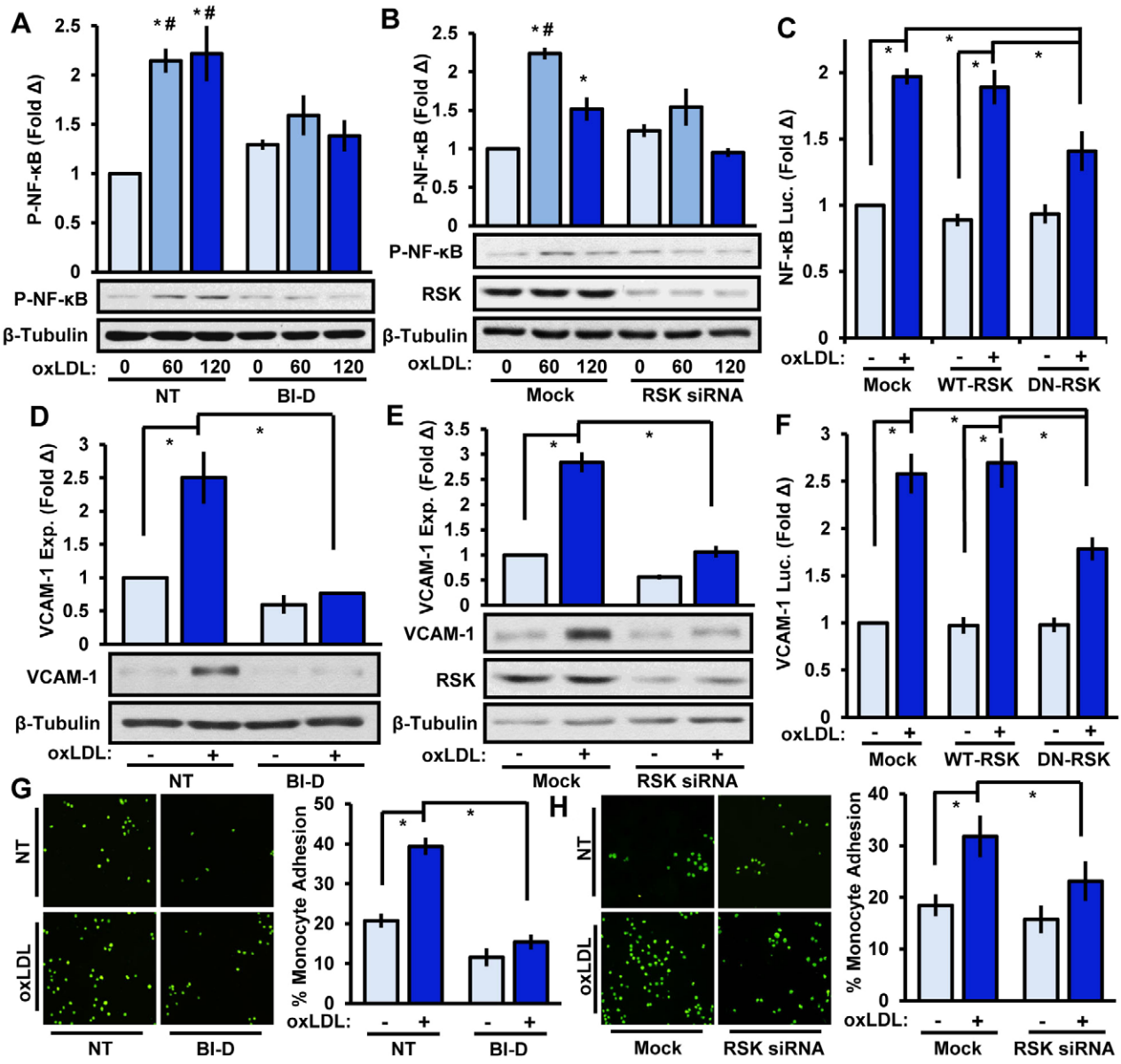

Fig. 3. RSK mediates oxLDL-induced NF-κB activation, VCAM-1 expression and monocyte adhesion. (A,B) Endothelial RSK signaling was inhibited with (A) BI-D1870 (BI-D, 5 µM, 1 h) or (B) RSK1 and RSK2 siRNA, and oxLDL (100 µg/ml)-induced NF-κB phosphorylation (P-NF-κB) was determined by immunoblotting after 60 or 120 min (n=4). (C) BAE cells were co-transfected with an SSRE-luciferase construct and either wild-type (WT)-RSK or dominant-negative (DN)-RSK constructs. OxLDL-induced luciferase (Luc.) activity was determined after 24 h (n=3). (D,E) RSK signaling in HAE cells was inhibited with (D) BI-D1870 (5 µM, 1 h) or (E) RSK1 and RSK2 siRNA and oxLDL-induced VCAM-1 expression was determined after 6 h by immunoblotting (n=4). (F) BAE cells were co-transfected with a VCAM-luciferase construct and either WT-RSK or DN-RSK constructs. OxLDL-induced luciferase (Luc.) activity was determined after 24 h (n=3). (G,H) RSK signaling in HAE cells was inhibited with (G) BI-D1870 (5 µM, 1 h) or (H) RSK1 and RSK2 siRNA, and oxLDL-induced monocyte adhesion was determined after 6 h using static adhesion assays (n=4). Results are mean±s.e.m. *P<0.05 (compared to 0 time or no treatment) or $^{\#}P$<0.05 (compared to respective timepoint) using two-way ANOVA with Bonferroni post-hoc test. NT, no treatment. Mock indicates mock transfection.

(FAK-WT) and FAK$^{KD/flox}$ (FAK-KD) mice were crossed with mice expressing Cre recombinase under the control of a tamoxifen-inducible, endothelial-cell-specific promoter. Upon tamoxifen feeding, FAK-KD (Cre+) mice are left with only the kinase-dead allele in the endothelium, whereas FAK-WT (Cre−), FAK-WT (Cre+) and FAK-KD (Cre−) mice all have wild-type FAK alleles remaining. At 7 weeks of age, all mice were given tamoxifen-containing food for 3 weeks. Subsequently, mice were fed a high-fat Western diet for 12 weeks to induce early atherosclerosis. We first confirmed the mouse model by staining for active FAK in the FAK-WT (Cre+) and FAK-KD (Cre+) mice and found that the FAK-KD (Cre+) mice displayed little to no FAK activity in the endothelial layer compared to the FAK-WT (Cre+) controls, whereas medial FAK activation remained unchanged (Fig. 6A–C). FAK-WT (Cre−), FAK-WT (Cre+) and FAK-KD (Cre−) showed a similar macrophage (Mac2 positive) area and total plaque size (Fig. 6D–F). However, FAK-KD (Cre+) mice exhibited a significantly reduced macrophage area and total plaque size (Fig. 6D–F). Loss of FAK activity in the endothelium did not affect mouse weight, total cholesterol, high-density lipoprotein cholesterol, LDL cholesterol, triglyceride levels or plasma cytokine levels,

Journal of Cell Science (2016) 129, 1580-1591 doi:10.1242/jcs.182097

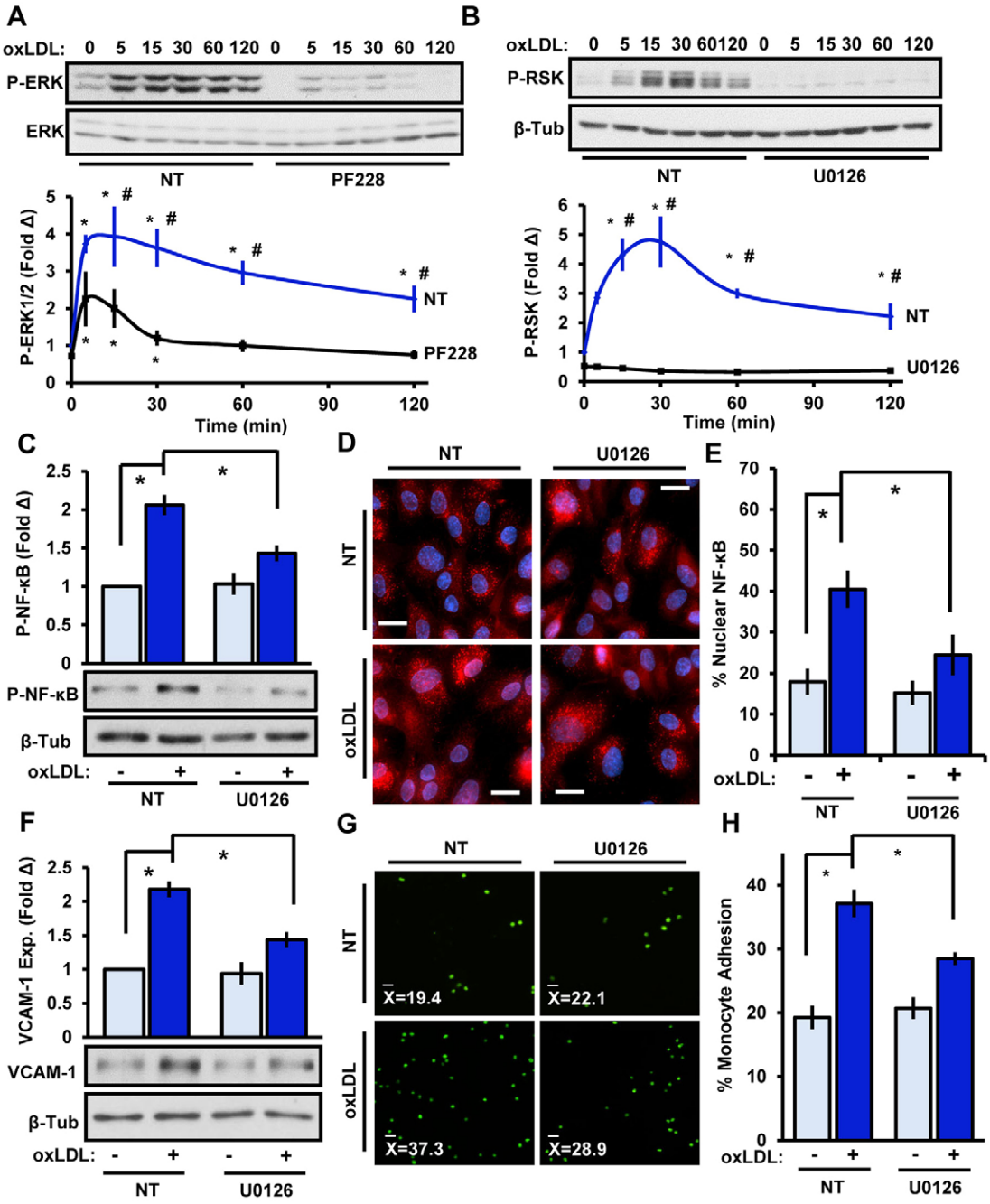

Fig. 4. FAK-dependent ERK1/2 signaling mediates RSK activation and proinflammatory signaling. (A) oxLDL-induced (100 µg/ml, indicated times) ERK activation was assessed in HAECs following treatment with the FAK inhibitor PF-573228 (PF228, 4 µM, 1 h). (B) ERK signaling in endothelial cells was reduced by pretreatment with the MEK1/2 inhibitor U0126 (10 µM, 1 h), and oxLDL-induced RSK signaling was assessed by immunoblotting (n=5). (C–H) Endothelial ERK1/2 signaling was reduced by using U0126, and oxLDL-induced (C) NF-κB phosphorylation (P-NF-κB, 1 h, n=5), (D,E) p65 nuclear localization (1 h, n=4), (F) VCAM-1 expression (exp., 6 h, n=4) and (G,H) monocyte adhesion (6 h, n=4) were assessed. Results are mean±s.e.m. *P<0.05 (compared to 0 time or no treatment) or $^{\#}P$<0.05 (compared to respective timepoint) using two-way ANOVA with Bonferroni post-hoc test. NT, no treatment.

suggesting that FAK activity modulates early atherosclerosis without affecting systemic risk factors (Tables S1–S3). Consistent with reduced atherosclerotic inflammation, FAK-KD (Cre+) mice showed significantly reduced levels of VCAM-1 expression and lower levels of active RSK (RSK phosphorylated at S380) compared to the FAK-WT controls (Fig. 7A,B). Taken together, our data demonstrates that FAK activity crucially regulates proinflammatory signaling, adhesion molecule expression and early atherosclerosis (Fig. 7C).

DISCUSSION

OxLDL drives NF-κB activation and VCAM-1 expression through integrin-α5β1-dependent FAK signaling; however, the mechanisms regulating FAK-dependent NF-κB signaling have remained elusive (Yurdagul et al., 2014). Here, we define a new signaling pathway involving FAK-dependent activation of the RSK pathway to promote NF-κB activation through its classic upstream mediator IKKβ. Although both RSK and NF-κB activation are known to be redox sensitive, we show that preventing integrin signaling or FAK

Journal of Cell Science (2016) 129, 1580-1591 doi:10.1242/jcs.182097

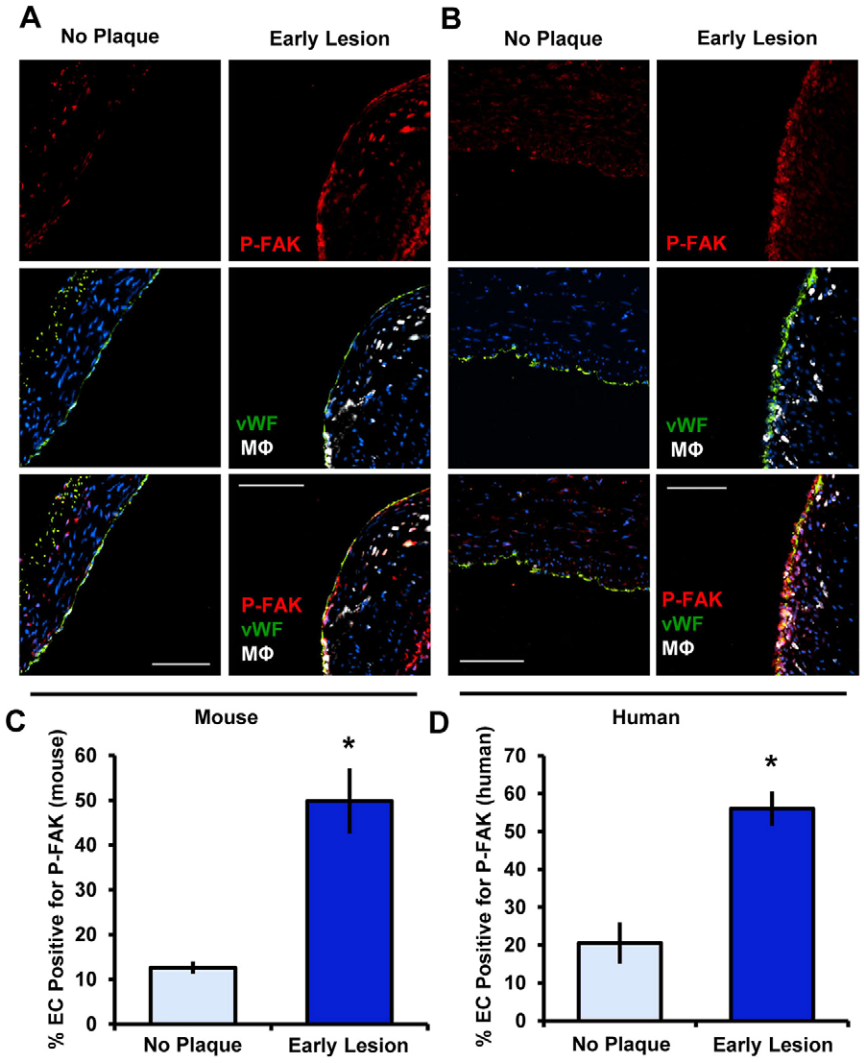

Fig. 5. FAK activation in endothelial cells is detected during early atherosclerosis. (A) Mouse lesions were immunostained for active FAK (P-Y397 FAK, red), endothelial cells (vWF, green), myeloid cells (Mac2; MΦ, white) and DAPI (blue) (n=4 for each group). (B) Human coronary arteries were immunostained for active FAK (P-FAK, red), endothelial cells (vWF, green), myeloid cells (CD68, MΦ, white) and DAPI (blue) (n=4 for each group). (C,D) Endothelial FAK phosphorylation in the mouse and human specimens was quantified as the percentage of the endothelial cell layer (EC, vWF positive) staining positive for P-FAK. Results are mean±s.e.m. *P<0.05 (compared to no plaque result) using two-tailed Student's t-test. Scale bars: 50 µm (A); 100 µm (B).

activation does not significantly affect oxLDL-induced ROS levels, suggesting that FAK-dependent activation of the RSK–IKKβ–NK-κB pathway operates independently from oxidative stress (Abe et al., 2000; Kabe et al., 2005). Instead, oxLDL drives FAK-dependent ERK activation that results in RSK-dependent signaling to IKKβ and NF-κB. We further demonstrate elevated FAK activation in the endothelium overlying both mouse and human atherosclerotic plaques, and show that transgenic mice containing an endothelial-specific and tamoxifen-inducible FAK-KD mutation are resistant to diet-induced RSK activation, VCAM-1 expression and macrophage accumulation. Taken together, these data demonstrate that RSK couples FAK signaling to NF-κB activation and critically regulates early atherosclerosis.

The role of FAK in mediating inflammatory responses is context-dependent and likely occurs through multiple pathways that form distinct multiprotein complexes. Integrin engagement to the extracellular matrix activates FAK, and multiple stimuli – including TNFα, disturbed flow and oxidized LDL – rapidly promote integrin-dependent FAK signaling (Lim et al., 2012; Petzold et al., 2009; Schlaepfer et al., 2007; Yurdagul et al., 2014). In all cases, FAK knockdown, inhibition or rendering FAK kinase dead, clearly reduces proinflammatory gene expression and endothelial cell activation. However, the mechanisms by which these stimuli regulate NF-κB and particularly IKKβ signaling had not been previously shown. Interestingly, physical interactions between RIP1 and FAK transforms TNFα-induced responses from proapoptotic to proinflammatory responses (Kurenova et al., 2004; Park et al., 2009a). However, our results demonstrate that depletion of RIP1 in endothelial cells does not affect oxLDL-induced NF-κB activation. Furthermore, whereas TNFα-induced proinflammatory gene expression was initially considered to require FAK-dependent NF-κB activation, it has since been shown that TNFα-induced NF-κB nuclear translocation, NF-κB–DNA binding and NF-κB S536 phosphorylation are unaffected by the absence of FAK (Funakoshi-Tago et al., 2003; Schlaepfer et al., 2007). Interestingly, inhibiting FAK activity by using small-molecule inhibitors or through expression of the kinase-dead form in cells results in FAK nuclear localization. In the nucleus, the FAK FERM (band 4.1, ezrin, radixin, moesin homology) domain binds directly to GATA4 and increases E3-ligase-dependent ubiquitylation and degradation (Lim et al., 2012). FAK-mediated ubiquitylation and degradation of GATA4 prevents TNFα-induced VCAM-1 expression. However, we did not observe any changes in nuclear FAK in response to oxLDL. In the context of shear stress, endothelial cells that lack FAK show non-impaired NF-κB nuclear localization but significant decreases in NF-κB S536 phosphorylation (Petzold et al., 2009). Our data suggests that FAK mediates NF-κB activation, VCAM-1 expression and monocyte adhesion through RSK-dependent IKKβ

Journal of Cell Science (2016) 129, 1580-1591 doi:10.1242/jcs.182097

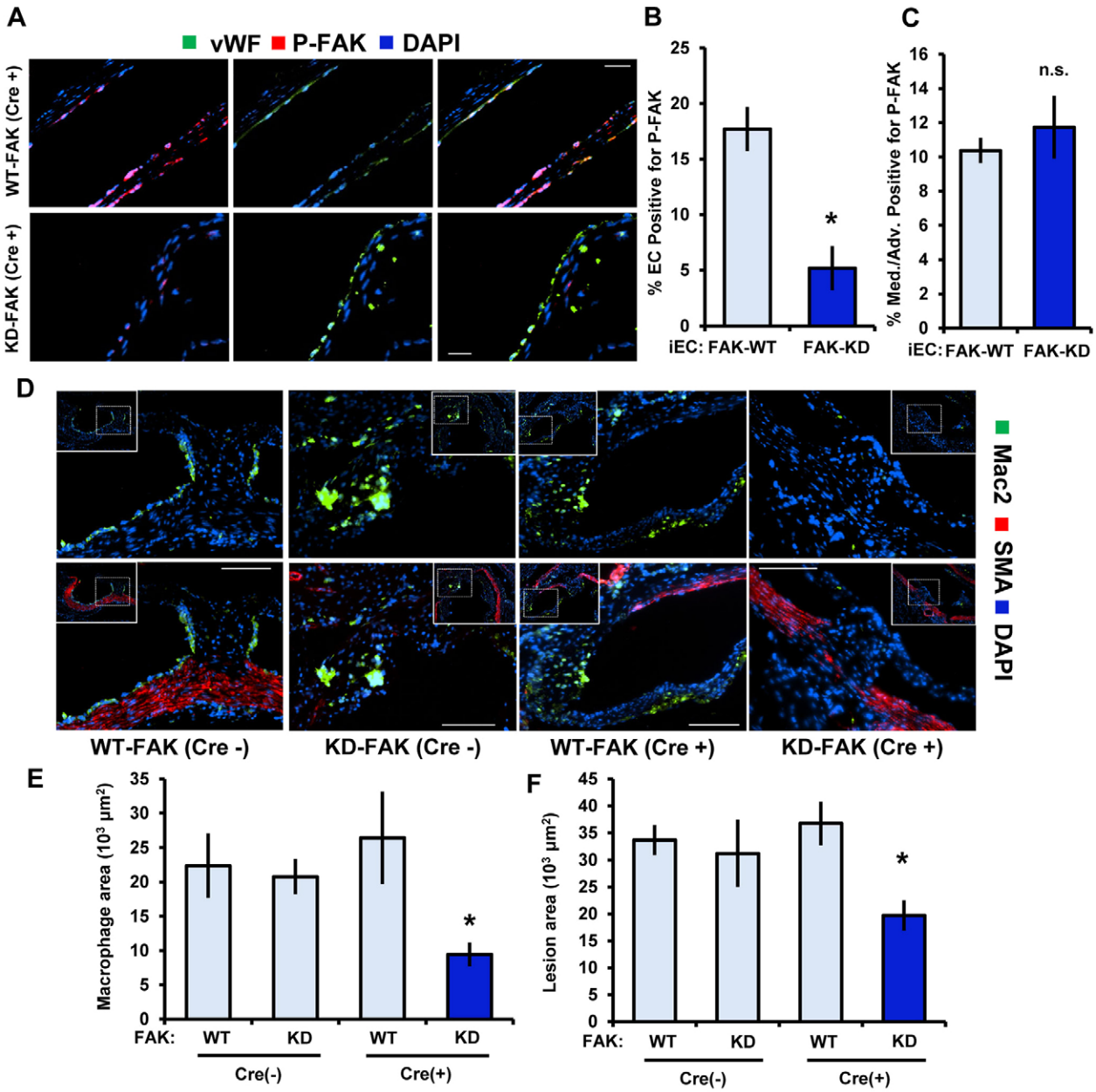

Fig. 6. FAK activation in endothelial cells is required for leukocyte recruitment in early atherosclerosis. (A) Aortic roots from FAK-WT (Cre+) and FAK-KD (Cre+) transgenic mice were immunostained for P-Y397 FAK (red), an endothelial cell marker (vWF, green) and DAPI. (B,C) P-FAK staining was quantified as the percentage of the endothelial cell layer (EC, vWF-positive) or the vessel media and adventitia staining positive for P-FAK. (D) Aortic root from transgenic mice was immunostained for myeloid cells (Mac2, green), smooth muscle cells (SMA, red) and DAPI. Representative micrographs are shown. (E) The Mac2-positive area was quantified from an average of three separate sites along the aortic root 50 µM away from each other. (F) Lesion size was quantified from neointima formation as an average of three separate sites along the aortic root 50 µM away from each other [n=6 for WT-FAK (Cre−), 5 for WT-FAK (Cre+), 7 for KD-FAK (Cre−) and 5 for KD-FAK (Cre+)]. Results are mean±s.e.m. *P<0.05 (compared to FAK-WT) using two-tailed Student's t-test. Scale bars: 20 µm (A); 50 µm (D).

signaling. However, whereas the decrease in early atherosclerosis seen in the FAK-KD transgenic mice *in vivo* correlates with reduced proinflammatory gene expression mediated by oxLDL *in vitro*, we cannot exclude the role of FAK inhibition on flow-induced endothelial cell activation or reduced TNFα-induced VCAM-1 expression. Therefore, loss of FAK kinase activity in endothelial cells likely reduces inflammatory responses by multiple mechanisms *in vivo*.

The RSK family of serine/threonine kinases participates in proliferation, survival and gene transcription (Anjum and Blenis, 2008). Structurally, RSK contains two kinase domains connected by a hydrophobic motif and a turn motif, and a D domain in the C-terminus that binds ERK1/2 (Romeo et al., 2012). Consistent with this, we show that inhibiting ERK1/2 reduces the amount of RSK activity induced by oxLDL. Oxidized LDL stimulates Y925 on FAK, a Grb2-binding site. Multiple stimuli induce Grb2–FAK interactions to mediate Ras- and SOS-dependent ERK1/2 activation. We provide new data showing that FAK-dependent ERK1/2 activation mediates oxLDL-induced NF-κB activation, VCAM-1 expression and monocyte binding. Although it is well-established that binding of ERK1/2 is required for complete RSK activation, we are the first to link FAK to ERK-dependent RSK

Journal of Cell Science (2016) 129, 1580-1591 doi:10.1242/jcs.182097

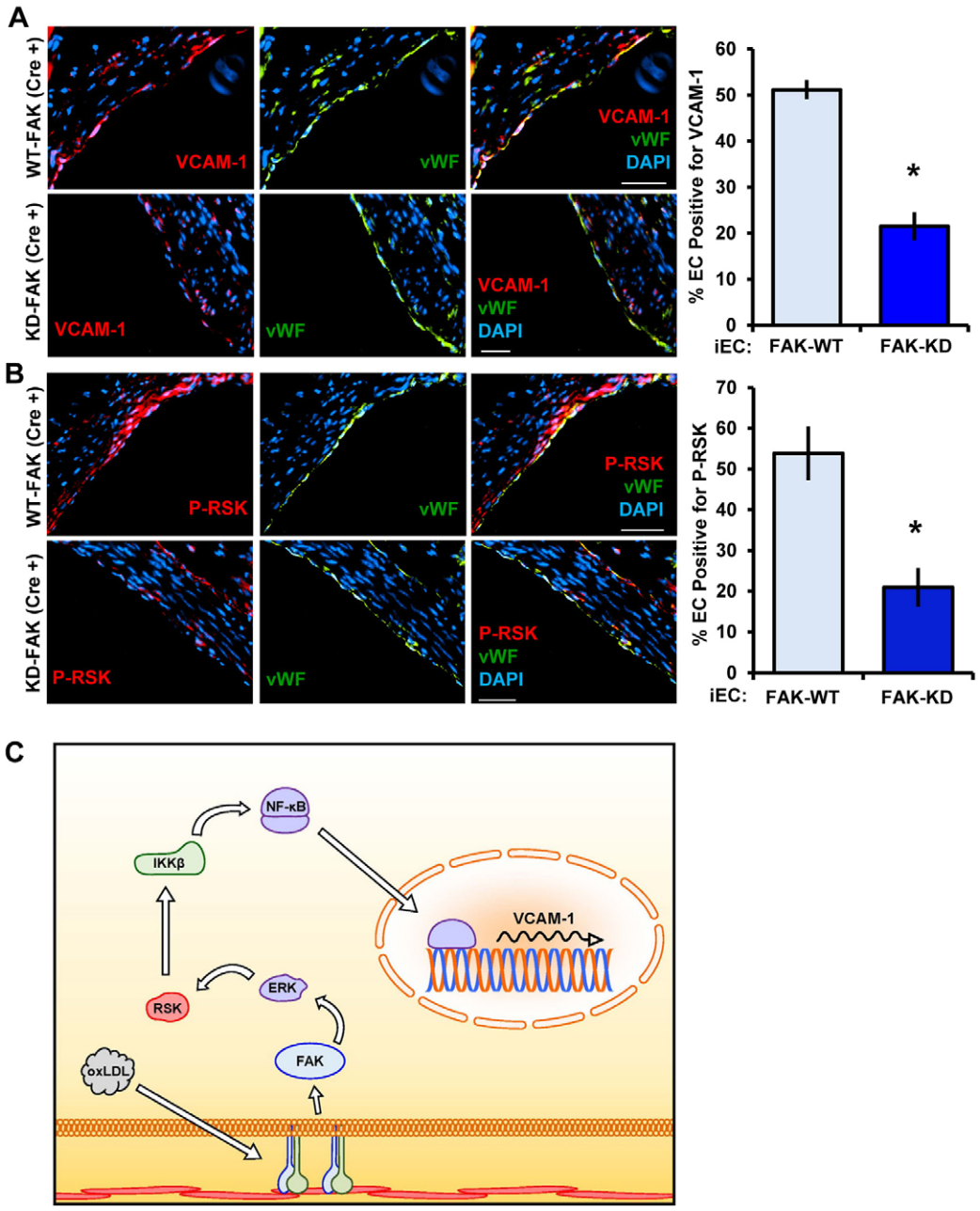

Fig. 7. FAK activation mediates VCAM-1 expression and RSK activation *in vivo*. Aortic roots from FAK-WT (Cre+) and FAK-KD (Cre+) mice were stained for (A) VCAM-1 (red) or (B) P-S380 RSK (red) and co-stained for endothelial cells (vWF, green) and DAPI. VCAM-1 or P-S380 RSK positive staining in the endothelium was quantified at three separate sites along the aortic root 50 µM away from each other (n=5 per group). Results are mean±s.e.m. *P<0.05 (compared to FAK-WT) using two-tailed Student's t-test. Scale bars: 50 µm. (C) Model of oxLDL-induced NF-kB activation through FAK-dependent RSK signaling.

activation and RSK downstream functions (Roux et al., 2003). RSK has been shown to affect multiple points along the canonical pathway leading to NF-κB activation. For instance, a candidate motif for RSK binding in IκBα exists (R-x-x-S) and precedes the key residue for IκBα ubiquitylation and degradation (S32). In fact, it has been demonstrated that IκBα is a RSK target, and RSK permits NF-κB activation by phosphorylating IκBα (Ghoda et al., 1997; Peng et al., 2010; Schouten et al., 1997). Alternatively, RSK also promotes p65 phosphorylation at S536, the site that is required for transcriptional activity and DNA processing (Bohuslav et al., 2004). However, it has also been reported that RSK binds directly to IKKβ and activates NF-κB in an IKKβ-dependent manner (Panta et al., 2004). Furthermore, persistent IKKβ activation by angiotensin II requires ERK1/2–RSK-dependent signaling, as blocking components of this pathway completely block IKKβ activation. Our data shows that inhibiting RSK diminishes oxLDL-induced IKKβ activation and that IKKβ knockdown inhibits oxLDL-induced NF-κB activation, excluding a role for RSK in directly influencing IκBα or NF-κB.

RSK signaling contributes to the pathogenesis of several vascular diseases. Turbulent blood flow, a crucial determinant of atherosclerosis, activates RSK *in vitro* and *in vivo*, and RSK signaling crucially governs flow-induced endothelial cell activation, controls nitric oxide bioavailability and promotes atherosclerotic

Journal of Cell Science (2016) 129, 1580-1591 doi:10.1242/jcs.182097

plaque formation (Heo et al., 2015). In addition, increased RSK activity can be observed in blood vessels belonging to diabetic mice, and inhibiting RSK increases endothelial nitric oxide synthase (eNOS, also known as NOS3) expression and restores vasodilation by acetylcholine (Le et al., 2013). Given that FAK also participates in flow-induced endothelial cell activation, it is possible that FAK mediates RSK activation in this system as well. Beyond atherosclerosis, RSK activity has also been associated with cardiomyopathies, and prolonged cardiac repolarization, a frequent cause of arrhythmias, is attributed to RSK-mediated inhibition of voltage-gated K^+ channels (Lu et al., 2008; Takeishi et al., 2002). RSK might also contribute to injury induced by myocardial infarction by promoting cardiac apoptosis through binding and phosphorylating ERK5 on S496 (Le et al., 2012). Although RSK1, RSK2 and RSK3 triple knockouts exist and are not embryonically lethal, little information has been gathered regarding phenotypes that relate to vascular biology.

Although FAK has been associated with endothelial NF-κB activation and proinflammatory gene expression, our data are the first to definitively link FAK signaling in endothelial cells to leukocyte recruitment and early atherosclerosis. Although our studies utilize cell-type-specific inhibition and point to a defined mechanism, FAK inhibitors could have complex effects on atherosclerosis. FAK-KD transgenic mice show reduced endothelial cell permeability compared to wild-type mice, which should decrease the infiltrating leukocyte population during the progression of atherosclerosis (Chen et al., 2012; Jean et al., 2014). Inhibiting FAK in smooth muscle cells results in decreased proliferation and motility, features that drive stenotic lesions but protect atherosclerotic plaques from rupturing. In addition, inhibiting FAK decreases motility in macrophages, which could limit targeting to the plaques but also egression out of the plaque (Abshire et al., 2011; Park et al., 2009b). Unfortunately, we cannot predict whether FAK signaling crucially regulates atherosclerosis after plaque formation, a clinically relevant timeframe, given that our model only addresses early disease development. However, loss of FAK activity in the endothelium *in vivo* correlates with decreased VCAM-1 expression and macrophage accumulation, crucial determinants for progression of atherosclerosis. Our data presented herein suggest that FAK and RSK inhibitors, currently in clinical trials targeting cancer, could be therapeutically beneficial in the treatment of atherosclerosis.

MATERIALS AND METHODS

Endothelial cell culture, transfections, and cytosol and nuclear separation

HAE cells (HAECs, Lonza) were purchased at passage 3 and maintained in MCDB 131 supplemented with 10% fetal bovine serum (FBS), 2 mM glutamine, 10 U/ml penicillin (GIBCO), 100 µg/ml streptomycin (GIBCO), 60 µg/ml heparin sodium and bovine brain extract (25 µg/ml, isolated from bovine hypothalamus, Pel-Freeze) and were used between passages 6 and 10. Experiments were performed on confluent endothelial cell monolayers in MCDB-131 containing 0.5% fetal bovine serum (FBS). HAECs at 75% confluency were transfected with SMARTpool siRNA oligonucleotides (GE Lifesciences) targeting either FAK (Cat# L-003164-00-0005), IKKβ (Cat# L-003503-00-0005), RIP1 (Cat# L-004445-00-0005), TAK1 (Cat# L-003790-00-0005), RSK1 (Cat# L-003025-00-0005), RSK2 (L-004663-00-0005) and NIK (Cat# L-003580-00-0005) (50 nM) using Lipofectamine 2000 (Life Technologies) for 2.5 h on two consecutive days and experiments were performed 2 days later. Bovine aortic endothelial cells maintained in Dulbecco's modified Eagle's medium (DMEM; Life Technologies) containing 10% FBS with glutamine were transfected with 1 µg of either wild-type RSK or dominant-negative RSK constructs per well in a six-well plate with co-transfection of either 1 µg of SSRE-luciferase or VCAM1-luciferase constructs per well using Lipofectamine 2000 for 2.5 h. Luciferase experiments were performed two days later in low-serum-containing media. Primary MLECs were isolated as described previously (Chen et al., 2012). Briefly, lungs were harvested, minced and then dissociated into single cells. Endothelial cells were isolated using magnetic beads coated with rat anti-mouse-CD31 (5 µg/100 µl beads, Cat# 553370, BD Biosciences) and -CD102 antibodies (5 µg/100 µl beads, Cat# 553326, BD Biosciences). All animal experiments were performed according to approved guidelines. Isolated endothelial cells were verified for Dil-Ac-LDL uptake (10 µg/ml, for 4 h) and for CD31 and ICAM-2 surface expression [using, respectively, FITC-conjugated rat anti-mouse-CD31 (1:100, Cat# 558738, BD Biosciences) and biotinylated rat anti-mouse ICAM-2 (1:100, Cat# 557441, BD Biosciences) antibodies]. MLECs were treated with adenoviral Cre to promote floxed FAK excision and used at passage <5 without immortalization. MLECs were maintained in EBM-2 basal EC medium (Lonza) with microvascular Bullet Kit supplementation (Lonza) and 10% FBS on plates coated with 0.2% gelatin and 10 µg/ml rat tail collagen I (Millipore). Subsequently, cells were placed under serum-free conditions for 4 h prior to experiments. Cytosol and nuclear separations were carried out according to the manufacturer's protocol (NE-PER, Thermo-Scientific).

Immunocytochemistry

Cells were fixed in 4% formaldehyde, permeabilized with 0.1% Triton X-100, blocked with 1% denatured bovine serum albumin (BSA) containing 10% goat serum and incubated with rabbit anti-NF-κB (p65 subunit) antibody overnight (1:200, sc-109, Santa Cruz). Cells were washed in TBS with 0.1% Tween 20 (TBST) and incubated with Alexa-Fluor-488-conjugated goat anti-rabbit-IgG secondary antibodies for 2 h. Unbound secondary antibody was removed by TBST wash, and coverslips were mounted onto microslides using Fluoromount G. Stains were visualized on a Nikon Eclipse Ti inverted epifluorescence microscope equipped with a Photometrics CoolSNAP120 ES2 camera and the NIS Elements 3.00, SP5 imaging software. Cells were scored for nuclear localization and at least 100 cells were counted per condition for each experiment.

Lentivirus production

HEK 293FT cells were transfected with lentiviral expression vectors and the Invitrogen ViraPower Lentiviral Packaging plasmids (pLP1, pLP2 and pLP/VSVG). Lentiviral particles were harvested 48 and 72 h post transfection. pLenti-GFP (Addgene), pCDH-GFP-FAK and constitutively active pCDH-FAK Y180A/M183A were used as previously described (Lietha et al., 2007; Chen et al., 2012).

Animals and tissue harvest

Animal protocols were approved by the LSU Health Sciences Center-Shreveport and by the University of California San Diego institutional animal care and use committee. All animals were cared for according to the National Institutes of Health guidelines for the care and use of laboratory animals. $ApoE^{-/-}$ mice on a C57BL6 background (8–10 weeks old) were placed on a high-fat Western diet (TD 88137, Harlan-Teklad) for 8 weeks before euthanasia. Mice were perfused with 4% formaldehyde by cardiac puncture in the left ventricle and brachiocephalic arteries were collected and processed for paraffin embedding. Mice with loxP sites flanking FAK exon 3 (FAK fl/fl) and a tamoxifen-inducible Cre–estrogen-receptor fusion protein [Cre-ER(T)] transgene downstream of the 5′ endothelial enhancer of the stem cell leukemia locus (Weis et al., 2008) were crossed with heterozygous mice containing a kinase-dead (FAK KD/WT) knock-in mutation within FAK exon 15 (NC_000081.6) (Lim et al., 2010). At 6 weeks of age, FAK fl/KD Cre-ER(T) (designated FAK-KD) and FAK fl/WT Cre-ER(T) (designated FAK-WT) littermates were treated with tamoxifen-containing chow (Harlan) for 3 weeks. Subsequently, mice were fed regular chow for 1 week, then an atherogenic diet (Harlan Teklad, TD 02028) for 12 weeks. Mice were then euthanized, and aortic roots were fixed and processed for paraffin embedding. Lesions were stained with antibodies targeting Mac2 (1:10,000, ACL8942F, Accurate Chemical & Scientific Co.), phosphorylated RSK (S380, 1:200, Cat# 3283, Cell Signaling Technologies), vonWillebrand factor (vWF, 1:100 dilution, Cat# ab11713, Abcam), phosphorylated FAK (Y397, 1:250 dilution, 3283, Cell Signaling

Technologies) and VCAM-1 (1:200; Cat# ab134047, Abcam) followed by incubations with Alexa-Fluor-conjugated secondary antibodies and quantified as either total area positive for macrophage staining or the percentage of endothelial cells positive for either phosphorylated RSK, phosphorylated FAK or VCAM-1. Total cholesterol, HDL cholesterol (Wako) and triglyceride levels (Pointe Scientific) were measured using commercially available kits. LDL was calculated using the Friedewald equation. All experiments using human tissue were deemed non-human research by the LSU Health Science Center – Shreveport Institutional Review Board due to the exclusive use of postmortem samples. Human tissue was excised postmortem during routine autopsy at the LSU Health Sciences Center-Shreveport, processed for paraffin embedding and classified according to the Stary system of atherosclerosis.

Immunoblotting, immunocytochemistry and proximity ligation assay

Cell lysis and immunoblotting was performed as previously described (Orr et al., 2005). Antibodies used included rabbit anti-NF-κB (p65 subunit, S536, Cat# 3033, 1:2000 dilution), rabbit anti-phosphorylated IκBα (S32, Cat# 2859, 1:1000 dilution), rabbit anti-phosphorylated ERK1/2 (Y202/Y204, Cat# 4370, 1:1000 dilution), rabbit anti-phosphorylated RSK (S380, Cat# 11989, 1:500 dilution), rabbit anti-RSK1/2/3 (Cat# 9355, 1:1000 dilution), rabbit anti-FAK (Cat# 3285, 1:1000 dilution), rabbit anti-phosphorylated FAK (Y397, Cat# 3283, 1:1000 dilution), rabbit anti-phosphorylated FAK (Y925, Cat# 3284, 1:1000 dilution), rabbit anti-β-Tubulin (Cat# 2146, 1:5000 dilution), rabbit anti-GAPDH (Cat# 5174, 1:5000 dilution) (Cell Signaling Technologies), rabbit anti-ERK1/2 (Cat# sc-94, 1:20,000 dilution), rabbit anti-RIP1 (Cat# sc-133102, 1:1000 dilution), rabbit anti-TAK1 (Cat# sc-7162, 1:1000 dilution), mouse anti-NIK (Cat# sc-7211, 1:500 dilution) and mouse anti-GST (Cat# sc-138, 1:1000 dilution) (Santa Cruz Biotechnology) and rabbit anti-VCAM-1 (Cat# ab134047, 1:1000 dilution) (Abcam). Densitometry was performed using ImageJ software. Proximity ligation assays (PLAs) were performed according to manufacturer's instructions. Briefly, cells were fixed in 4% formaldehyde for 20 min, permeabilized with 0.1% Triton X-100, and blocked with 1% denatured bovine serum albumin (BSA) containing 10% goat serum. Primary antibodies to Grb2 (mouse, 1:1000, Cat# G2791, Sigma) and FAK (rabbit, 1:1000, Cat# 3285, Cell Signaling Technologies) were placed on coverslips and incubated overnight. Cells were then washed five times with TBST and the PLA (Olink Bioscience) assay was performed. Cells were then treated with DAPI and Alexa-Fluor-488–phalloidin (Life Technologies) then mounted onto microscope slides using Fluoromount G. Stains were visualized on a Nikon Eclipse Ti inverted epifluorescence microscope equipped with a Photometrics CoolSNAP120 ES2 camera and the NIS Elements 3.00, SP5 imaging software. Cells were scored for dots per cell and at least 100 cells were counted per condition for each experiment.

Immunoprecipitations and IKK kinase assay

Cells were treated as described and then rinsed once with ice-cold 1× PBS. The PBS was removed and then cells were lysed with cold immunoprecipitation lysis buffer (20 mM Tris-HCl pH 7.5, 150 mM NaCl, 1 mM EDTA, 1 mM EGTA, 1% Triton X-100, 1× protease inhibitor cocktail, 1× phosphatase inhibitor cocktail) and immunoprecipitated with antibodies targeting mouse anti-Grb2 (Sigma-Aldrich) or rabbit anti-FAK (Cell Signaling Technologies) for 4 h. These were incubated with 50 µl of 1× or 2× Protein-A–Sepharose bead slurry (GE Healthcare) for 2 h and rinsed three times followed by addition of 2× Laemmli buffer. For IKK kinase assays, immunoprecipitations were performed by incubating lysates with an anti-IKKβ antibody (1:100) for 3 h followed by incubation with 50 µl of 1× or 2× Gammabind G bead slurry for 2 h. Beads were washed three times with immunoprecipitation lysis buffer and once in kinase buffer (25 mM Tris-HCl pH 7.5, 5 mM β-glycerophosphate, 2 mM DTT, 0.1 mM Na_3VO_4 and 10 mM $MgCl_2$). ATP (200 µM) and 1 µg of recombinant GST–IκBα was then added and the kinase reaction was allowed to proceed for 30 min at 30°C. The reaction was stopped by the addition of 2× Laemmli buffer. The lysates were then run on an SDS-PAGE gel and IKK activity was detected using a phospho-specific antibody to IκBα (Cat# 2859, Cell Signaling Technologies, 1:1000).

Monocyte adhesion assay

Human THP-1 monocytes were labeled with Cell Tracker Green (Life Technologies) according to the manufacturer's protocol. HAEC monolayers were treated as described and 10^6 monocytes were added per well of a 24-well plate (~5:1 ratio of monocytes to endothelial cells). Monocytes were allowed to attach for 10 min at 37°C in HBSS containing Ca^{2+} and Mg^{2+}. Supernatant and two washes were collected as the non-attached fraction, and both adherent and non-adherent monocytes were then lysed in 100 mM NaOH. Fluorescence at 488 nm was quantified using a FLUOstar Optima fluorescence plate reader, and results were normalized to un-bound fraction and expressed as the percent of monocytes adhering.

Reactive oxygen species

HAECs were cultured in phenol-red-free media then loaded with 10 µM DCFDA for 45 min and treated with oxLDL for various times. Cells were then read on a FLUOstar plate reader and arbitrary units were quantified as fold changes.

Cytokine array

Mouse plasma was assayed using a mouse cytokine array panel according to the manufacturer's protocol (R&D systems, MN). Cytokine arrays were imaged and densitometry values were calculated using Image Lab software (Biorad, CA). Cytokine values were then compared between the control and kinase-dead groups using a Student's *t*-test with a 95% confidence interval to identify significance.

Statistical analysis

Statistical comparisons between groups were performed using GraphPad Prism software. Data was tested for normality (Kolmogorov–Smirnov test) and data that passed the normality assumption was analyzed by using a Student's *t*-test, one-way ANOVA with Newman–Keuls post-test or two-way ANOVA with Bonferroni post-tests. Data that failed the normality assumption were analyzed by using the non-parametric Mann–Whitney U test and the Kruskal–Wallis test with post-hoc analysis. Error bars indicate s.e.m.

Acknowledgements

The authors would like to thank David Krzywanski (LSUHSC-Shreveport, Shreveport, LA) for providing THP-1 monocytes and Jun-Ichi Abe (The University of Texas MD Anderson Cancer Center, Houston, TX) for providing the wild-type and dominant-negative RSK constructs.

Competing interests

The authors declare no competing or financial interests.

Author contributions

A.Y.J., F.J.S., X.L.C. and C.B.P. performed experiments. A.Y.J., F.J.S., D.D.S. and A.W.O. designed experiments. A.Y.J. and A.W.O. wrote the manuscript and all authors contributed to the preparation of the manuscript.

Funding

This work was supported by the National Institutes of Health [grant numbers R01 HL098435 to A.W.O., RO1 CA180769 and RO1 CA102310 to D.D.S., T32 CA121938 to F.J.S.]; by the American Heart Association [grant numbers 15GRNT25560056 to A.W.O., 15SDG25710038 to C.B.P., 14PRE18660003 to A.Y.J.]; and by the Louisiana Board of Regents [grant number LEQSF (2008–13)-FG-20 to A.Y.J.]. Deposited in PMC for release after 12 months.

Supplementary information

Supplementary information available online at
http://jcs.biologists.org/lookup/suppl/doi:10.1242/jcs.182097/-/DC1

References

Abe, J.-i., Okuda, M., Huang, Q., Yoshizumi, M. and Berk, B. C. (2000). Reactive oxygen species activate p90 ribosomal S6 kinase via Fyn and Ras. *J. Biol. Chem.* **275**, 1739-1748.

Abshire, M. Y., Thomas, K. S., Owen, K. A. and Bouton, A. H. (2011). Macrophage motility requires distinct alpha5beta1/FAK and alpha4beta1/paxillin signaling events. *J. Leukoc. Biol.* **89**, 251-257.

Anjum, R. and Blenis, J. (2008). The RSK family of kinases: emerging roles in cellular signalling. *Nat. Rev. Mol. Cell Biol.* **9**, 747-758.

Bohuslav, J., Chen, L.-f., Kwon, H., Mu, Y. and Greene, W. C. (2004). p53 induces NF-kappaB activation by an IkappaB kinase-independent mechanism involving phosphorylation of p65 by ribosomal S6 kinase 1. *J. Biol. Chem.* **279**, 26115-26125.

Chen, X. L., Nam, J.-O., Jean, C., Lawson, C., Walsh, C. T., Goka, E., Lim, S.-T., Tomar, A., Tancioni, I., Uryu, S. et al. (2012). VEGF-induced vascular permeability is mediated by FAK. *Dev. Cell* **22**, 146-157.

Funakoshi-Tago, M., Sonoda, Y., Tanaka, S., Hashimoto, K., Tago, K., Tominaga, S. and Kasahara, T. (2003). Tumor necrosis factor-induced nuclear factor kappaB activation is impaired in focal adhesion kinase-deficient fibroblasts. *J. Biol. Chem.* **278**, 29359-29365.

Ghoda, L., Lin, X. and Greene, W. C. (1997). The 90-kDa ribosomal S6 kinase (pp90rsk) phosphorylates the N-terminal regulatory domain of IkappaBalpha and stimulates its degradation in vitro. *J. Biol. Chem.* **272**, 21281-21288.

Gloire, G., Legrand-Poels, S. and Piette, J. (2006). NF-kappaB activation by reactive oxygen species: fifteen years later. *Biochem. Pharmacol.* **72**, 1493-1505.

Goyal, T., Mitra, S., Khaidakov, M., Wang, X., Singla, S., Ding, Z., Liu, S. and Mehta, J. L. (2012). Current concepts of the role of oxidized LDL receptors in atherosclerosis. *Curr. Atheroscler. Rep.* **14**, 150-159.

Heo, K.-S., Le, N.-T., Cushman, H. J., Giancursio, C. J., Chang, E., Woo, C.-H., Sullivan, M. A., Taunton, J., Yeh, E. T. H., Fujiwara, K. et al. (2015). Disturbed flow-activated p90RSK kinase accelerates atherosclerosis by inhibiting SENP2 function. *J. Clin. Invest.* **125**, 1299-1310.

Jean, C., Chen, X. L., Nam, J.-O., Tancioni, I., Uryu, S., Lawson, C., Ward, K. K., Walsh, C. T., Miller, N. L. G., Ghassemian, M. et al. (2014). Inhibition of endothelial FAK activity prevents tumor metastasis by enhancing barrier function. *J. Cell Biol.* **204**, 247-263.

Kabe, Y., Ando, K., Hirao, S., Yoshida, M. and Handa, H. (2005). Redox regulation of NF-kappaB activation: distinct redox regulation between the cytoplasm and the nucleus. *Antioxid. Redox Signal.* **7**, 395-403.

Kurenova, E., Xu, L.-H., Yang, X., Baldwin, A. S., Jr., Craven, R. J., Hanks, S. K., Liu, Z.-G. and Cance, W. G. (2004). Focal adhesion kinase suppresses apoptosis by binding to the death domain of receptor-interacting protein. *Mol. Cell. Biol.* **24**, 4361-4371.

Lawrence, T. (2009). The nuclear factor NF-kappaB pathway in inflammation. *Cold Spring Harb. Perspect. Biol.* **1**, a001651.

Le, N.-T., Takei, Y., Shishido, T., Woo, C.-H., Chang, E., Heo, K.-S., Lee, H., Lu, Y., Morrell, C., Oikawa, M. et al. (2012). p90RSK targets the ERK5-CHIP ubiquitin E3 ligase activity in diabetic hearts and promotes cardiac apoptosis and dysfunction. *Circ. Res.* **110**, 536-550.

Le, N.-T., Heo, K.-S., Takei, Y., Lee, H., Woo, C.-H., Chang, E., McClain, C., Hurley, C., Wang, X., Li, F. et al. (2013). A crucial role for p90RSK-mediated reduction of ERK5 transcriptional activity in endothelial dysfunction and atherosclerosis. *Circulation* **127**, 486-499.

Libby, P., Ridker, P. M. and Hansson, G. K. (2011). Progress and challenges in translating the biology of atherosclerosis. *Nature* **473**, 317-325.

Lietha, D., Cai, X., Ceccarelli, D. F., Li, Y., Schaller, M. D. and Eck, M. J. (2007). Structural basis for the autoinhibition of focal adhesion kinase. *Cell* **129**, 1177-1187.

Lim, S.-T., Chen, X. L., Tomar, A., Miller, N. L. G., Yoo, J. and Schlaepfer, D. D. (2010). Knock-in mutation reveals an essential role for focal adhesion kinase activity in blood vessel morphogenesis and cell motility-polarity but not cell proliferation. *J. Biol. Chem.* **285**, 21526-21536.

Lim, S.-T., Miller, N. L. G., Chen, X. L., Tancioni, I., Walsh, C. T., Lawson, C., Uryu, S., Weis, S. M., Cheresh, D. A. and Schlaepfer, D. D. (2012). Nuclear-localized focal adhesion kinase regulates inflammatory VCAM-1 expression. *J. Cell Biol.* **197**, 907-919.

Lu, Z., Abe, J.-i., Taunton, J., Lu, Y., Shishido, T., McClain, C., Yan, C., Xu, S. P., Spangenberg, T. M. and Xu, H. (2008). Reactive oxygen species-induced activation of p90 ribosomal S6 kinase prolongs cardiac repolarization through inhibiting outward K+ channel activity. *Circ. Res.* **103**, 269-278.

Orr, A. W., Sanders, J., Bevard, M., Coleman, E., Sarembock, I. and Schwartz, M. (2005). The subendothelial extracellular matrix modulates NF-kappaB activation by flow: a potential role in atherosclerosis. *J. Cell Biol.* **169**, 191-202.

Panta, G. R., Kaur, S., Cavin, L. G., Cortes, M. L., Mercurio, F., Lothstein, L., Sweatman, T. W., Israel, M. and Arsura, M. (2004). ATM and the catalytic subunit of DNA-dependent protein kinase activate NF-kappaB through a common MEK/extracellular signal-regulated kinase/p90rsk signaling pathway in response to distinct forms of DNA damage. *Mol. Cell. Biol.* **24**, 1823-1835.

Park, S., Hatanpaa, K. J., Xie, Y., Mickey, B. E., Madden, C. J., Raisanen, J. M., Ramnarain, D. B., Xiao, G., Saha, D., Boothman, D. A. et al. (2009a). The receptor interacting protein 1 inhibits p53 induction through NF-kappaB activation and confers a worse prognosis in glioblastoma. *Cancer Res.* **69**, 2809-2816.

Park, Y. M., Febbraio, M. and Silverstein, R. L. (2009b). CD36 modulates migration of mouse and human macrophages in response to oxidized LDL and may contribute to macrophage trapping in the arterial intima. *J. Clin. Invest.* **119**, 136-145.

Peng, C., Cho, Y.-Y., Zhu, F., Xu, Y.-M., Wen, W., Ma, W.-Y., Bode, A. M. and Dong, Z. (2010). RSK2 mediates NF-{kappa}B activity through the phosphorylation of IkappaBalpha in the TNF-R1 pathway. *FASEB J.* **24**, 3490-3499.

Petzold, T., Orr, A. W., Hahn, C., Jhaveri, K. A., Parsons, J. T. and Schwartz, M. A. (2009). Focal adhesion kinase modulates activation of NF-kappaB by flow in endothelial cells. *Am. J. Physiol. Cell Physiol.* **297**, C814-C822.

Robbesyn, F., Salvayre, R. and Negre-Salvayre, A. (2004). Dual role of oxidized LDL on the NF-kappaB signaling pathway. *Free Radic. Res.* **38**, 541-551.

Romeo, Y., Zhang, X. and Roux, P. P. (2012). Regulation and function of the RSK family of protein kinases. *Biochem. J.* **441**, 553-569.

Roux, P. P., Richards, S. A. and Blenis, J. (2003). Phosphorylation of p90 ribosomal S6 kinase (RSK) regulates extracellular signal-regulated kinase docking and RSK activity. *Mol. Cell. Biol.* **23**, 4796-4804.

Schlaepfer, D. D., Hou, S., Lim, S.-T., Tomar, A., Yu, H., Lim, Y., Hanson, D. A., Uryu, S. A., Molina, J. and Mitra, S. K. (2007). Tumor necrosis factor-alpha stimulates focal adhesion kinase activity required for mitogen-activated kinase-associated interleukin 6 expression. *J. Biol. Chem.* **282**, 17450-17459.

Schouten, G. J., Vertegaal, A. C. O., Whiteside, S. T., Israël, A., Toebes, M., Dorsman, J. C., van der Eb, A. J. and Zantema, A. (1997). IkappaB alpha is a target for the mitogen-activated 90kDa ribosomal S6 kinase. *EMBO J.* **16**, 3133-3144.

Sun, S.-C. (2011). Non-canonical NF-kappaB signaling pathway. *Cell Res.* **21**, 71-85.

Sun, Z. and Andersson, R. (2002). NF-kappaB activation and inhibition: a review. *Shock* **18**, 99-106.

Takada, Y., Mukhopadhyay, A., Kundu, G. C., Mahabeleshwar, G. H., Singh, S. and Aggarwal, B. B. (2003). Hydrogen peroxide activates NF-kappa B through tyrosine phosphorylation of I kappa B alpha and serine phosphorylation of p65: evidence for the involvement of I kappa B alpha kinase and Syk protein-tyrosine kinase. *J. Biol. Chem.* **278**, 24233-24241.

Takeishi, Y., Huang, Q., Abe, J.-i., Che, W., Lee, J.-D., Kawakatsu, H., Hoit, B. D., Berk, B. C. and Walsh, R. A. (2002). Activation of mitogen-activated protein kinases and p90 ribosomal S6 kinase in failing human hearts with dilated cardiomyopathy. *Cardiovasc. Res.* **53**, 131-137.

Tanigawa, H., Miura, S.-i., Zhang, B., Uehara, Y., Matsuo, Y., Fujino, M., Sawamura, T. and Saku, K. (2006). Low-density lipoprotein oxidized to various degrees activates ERK1/2 through Lox-1. *Atherosclerosis* **188**, 245-250.

Valente, A. J., Irimpen, A. M., Siebenlist, U. and Chandrasekar, B. (2014). OxLDL induces endothelial dysfunction and death via TRAF3IP2: inhibition by HDL3 and AMPK activators. *Free Radic. Biol. Med.* **70**, 117-128.

Weis, S. M., Lim, S.-T., Lutu-Fuga, K. M., Barnes, L. A., Chen, X. L., Göthert, J. R., Shen, T.-L., Guan, J.-L., Schlaepfer, D. D. and Cheresh, D. A. (2008). Compensatory role for Pyk2 during angiogenesis in adult mice lacking endothelial cell FAK. *J. Cell Biol.* **181**, 43-50.

Xu, S., Ogura, S., Chen, J., Little, P. J., Moss, J. and Liu, P. (2013). LOX-1 in atherosclerosis: biological functions and pharmacological modifiers. *Cell. Mol. Life Sci.* **70**, 2859-2872.

Yurdagul, A., Jr., Green, J., Albert, P., McInnis, M. C., Mazar, A. P. and Orr, A. W. (2014). alpha5beta1 integrin signaling mediates oxidized low-density lipoprotein-induced inflammation and early atherosclerosis. *Arterioscler. Thromb. Vasc. Biol.* **34**, 1362-1373.